Solar Energy Materials & Solar Cells 117 (2013) 471–475

Contents lists available at ScienceDirect

Solar Energy Materials & Solar Cells

journal homepage: www.elsevier.com/locate/solmat

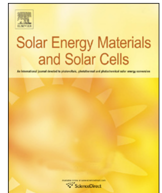

Crystal defects and their impact on ribbon growth on substrate (RGS) silicon solar cells

U. Hess [a,*], P.Y. Pichon [b], S. Seren [a], A. Schönecker [b], G. Hahn [a]

[a] *University of Konstanz, Department of Physics, P.O. Box X916, 78457 Konstanz, Germany*
[b] *RGS Development B.V., P.O. Box 40, 1724ZG Oudkarspel, The Netherlands*

ARTICLE INFO

Article history:
Received 3 May 2013
Received in revised form
10 July 2013
Accepted 12 July 2013
Available online 6 August 2013

Keywords:
Ribbon growth on substrate
Multicrystalline silicon
Solar cells
Crystal defects

ABSTRACT

Ribbon Growth on Substrate (RGS) silicon wafers are casted directly from the silicon melt onto reusable substrates. Material losses by wafer sawing are omitted and high production speeds can be achieved. However, multicrystalline RGS silicon as it is produced today incorporates high densities of crystal defects and impurities limiting the efficiency of the corresponding solar cells. The local impact of crystal defects on material quality is estimated via models developed by Donolato and Micard et al.. By theoretically negating the impact of grain boundaries and dislocations, charge carrier diffusion lengths are still limited to values $<100\,\mu$m. In addition to crystal defects which are common in other multicrystalline silicon materials, we found current collecting structures within grain boundaries. These structures can be associated with carbon and oxygen precipitation and are the cause for shunting phenomena. We conclude that high impurity concentrations are the dominant factor for limiting the performance of RGS silicon solar cells.

© 2013 Elsevier B.V. All rights reserved.

1. Introduction

By decoupling of wafer pulling and crystallization direction, Ribbon Growth on Substrate (RGS) [1] silicon wafers can be cast with a production speed in the order of one wafer per second. Kerf-less wafering can lead to a substantial cost reduction for solar cells [2]. The RGS wafers presented in this paper are produced by RGS Development on a laboratory scale R&D machine located at ECN (Netherlands). Using a screen-printing based cell process, the highest efficiency reported is $\eta = 13.1\%$ [3] (cell size: 5×5 cm^2). One of the most influential factors on cell performance is the low shunt resistance, with strongly fluctuating values in the range of 100–1000 Ω cm^2. For the further development of the RGS technology, understanding the cause of the varying shunt resistance and to overcome this limitation would result in a strong improvement of the quality of the wafers.

RGS material quality is decreased by several crystal defects. Grain sizes are in the order of 50–500 μm. The dislocation densities are in the range of 10^5–10^7/cm^2. For the microscopy image in Fig. 1, a cross-section of a RGS wafer was mechanically polished and treated with Secco etch [4]. The columnar grain structure as well as etch pits (small black dots) is observable, revealing the location of dislocations. Due to the casting method, defect-rich layers (thickness ~20 μm) are present on both wafer surfaces.

Impurity concentrations as measured by Fourier-transform infra-red spectroscopy (FTIR) for substitutional carbon [C_s] are above 10^{18}/cm^3 and for interstitial oxygen [O_i] $>10^{17}$/cm^3. The actual concentrations are higher, since e.g. precipitates are not detected. The minority charge carrier lifetime in p-type boron doped (3 Ω cm) as-grown wafers is in the order of ~1 μs. After cell processing steps like phosphorus gettering (emitter diffusion) and hydrogenation (SiN_x:H deposition and firing), the lifetime increases to values of about 5–10 μs in RGS wafers. The diffusion length of minority charge carriers is in the range of 60–90 μm, as determined from internal quantum efficiency (IQE) measurements.

To evaluate the impact of different crystal defects on the material quality, several measurement methods were used and the results correlated. Light Beam Induced Current (LBIC), Lock-In Thermography (LIT) and Photoluminescence (PL) were chosen as spatially resolved measurement methods for the characterization on cell level. Subsequently, the characterized solar cells were etched and the surfaces were mechanically polished (prior to the cell process, the defect-rich surfaces were already removed by acidic etching). Scanning Electron Microscopy (SEM), optical- as well as infrared-microscopy were used to investigate crystal defects. To detect the concentrations of metallic impurities high resolution Inductively Coupled Plasma Mass Spectroscopy (ICP MS) measurements were carried out.

* Corresponding author. Tel.: +49 7531 882060; fax: +49 7531 883895.
E-mail address: uwe.hess@uni-konstanz.de (U. Hess).

0927-0248/$ - see front matter © 2013 Elsevier B.V. All rights reserved.
http://dx.doi.org/10.1016/j.solmat.2013.07.019

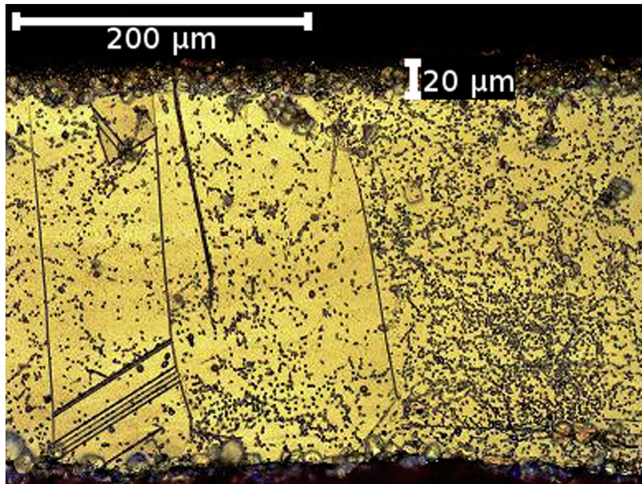

Fig. 1. Optical microscopy image of a polished cross-section of a RGS wafer treated with Secco etch.

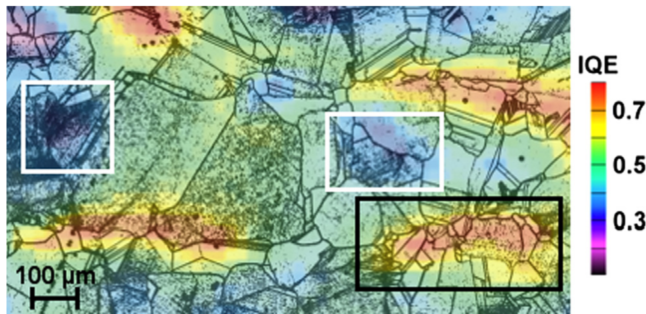

Fig. 2. Overlay of a LBIC scan (λ=980 nm, resolution: 25 μm) with the optical microscopy image of the corresponding polished and Secco-etched wafer. Defective regions (white rectangles) and a feature that is associated with a current collecting structure (black rectangle, structure has measured IQE values of >0.7) are highlighted.

2. Results

Fig. 2 shows a section of the overlay of a LBIC scan (980 nm wavelength) and the optical microscopy image of the corresponding polished and Secco-etch treated wafer. The accurateness of the overlay is in the order of the LBIC pixel width (25 μm). Like the highlighting in Fig. 2 indicates, the IQE is locally and distinctively varying from the average value. The following subsections are dealing with the different features of these overlay images.

2.1. Grain boundaries

As can be observed in Fig. 2, grain boundaries can show different behaviors in terms of short-circuit current or IQE. Several models were proposed to theoretically describe the recombinative behavior of grain boundaries [5]. However, these would require detailed knowledge of trapping and capture cross-sections of charge carriers at the grain boundary. Due to the grain size and distribution, corresponding measurements would be problematic.

To circumvent this problem, a method developed by Micard et al. [6] is used. This method uses a high-resolution LBIC line scan over grain boundaries. By theoretical considerations, the recombinative behavior of a grain boundary can be described by an effective surface recombination velocity S_{GB}. A defective region including several grain boundaries, whereby the influence of an isolated one cannot be distinguished, can also be described by an effective S_{GB} by the same model. For the evaluation on RGS samples, an exploitable drop in short-circuit current is only observable in defective regions. The majority (90%) of all investigated defective regions show varying S_{GB} in the range of 1000–50,000 cm/s. Single grain boundaries do rarely show such a distinctive behavior. Due to measurement noise, it can only be stated that the effective surface recombination velocities of most isolated grain boundaries are in the range below ~1000 cm/s. In grains with a size of several diffusion lengths and not being located in the vicinity of defective regions, recombination at grain boundaries has no dominant influence on material quality. This circumstance is also used in the next subsection for evaluation of the impact of dislocations.

2.2. Dislocations

To estimate the recombinative behavior of dislocations in RGS, a model developed by Donolato is used [7]. This theoretical consideration allows a correlation of the average normalized line recombination velocity Γ of dislocations, the charge carrier diffusion length and the so-called background diffusion length, which corresponds to the diffusion length if no dislocation would be present. On multicrystalline material, this model was successfully applied by Rinio et al. [8]. To apply this model to RGS several assumptions have to be made.

Due to the ratio of diffusion length (<100 μm) to cell thickness (220–250 μm), the cell can be approximately treated as a semi-infinite semiconductor. Since no preferred orientation of dislocations could be observed, a random orientation with an average angle of 45° between dislocations and surface is assumed. Since the influence of grain boundaries on the evaluation has to be minimized, determination of dislocation density and local diffusion length is narrowed to regions in the center of grains with a size of at least five times the diffusion length and with no defective region in the vicinity. Due to these criteria, only ~150 measurement points could be obtained from the investigated cell.

The dislocation density is determined by counting of etch pits on the Secco-etched wafer and the local diffusion length is determined by LBIC measurements with three different wavelengths (λ=833, 910, 980 nm) and a subsequent fit according to Basore [9]. Fig. 3 shows the obtained results.

Concerning the error margins, etch pit density determination and density variability within a grain lead to an uncertainty in the order of 10–20%. Above a density of 10^7/cm^2 the determination was increasingly unreliable. Due to the method of determining the local diffusion length, an error margin of about 5 μm has to be assumed.

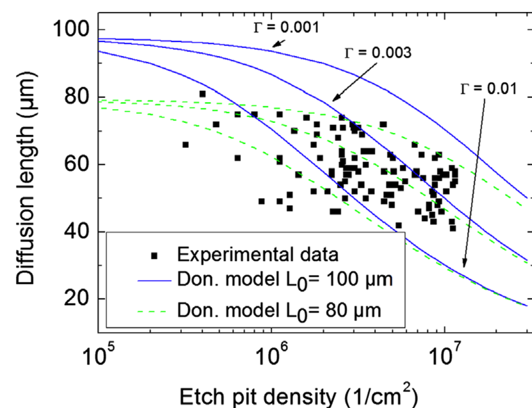

Fig. 3. The dashed green and the solid blue curves serve as guide to the eye for the theoretical Donolato model with two different background diffusion lengths L_0 and three different line recombination velocity values, each. The experimental data is gained by local determination of etch pit density and diffusion length. (For interpretation of the references to color in this figure caption, the reader is referred to the web version of this article.)

Download English Version:

https://daneshyari.com/en/article/6536377

Download Persian Version:

https://daneshyari.com/article/6536377

Daneshyari.com